

## A new behaviour of ac losses in superconducting $\text{Bi}_2\text{Sr}_2\text{CaCu}_2\text{O}_8$ single crystals

This article has been downloaded from IOPscience. Please scroll down to see the full text article.

2009 J. Phys.: Condens. Matter 21 045704

(<http://iopscience.iop.org/0953-8984/21/4/045704>)

View [the table of contents for this issue](#), or go to the [journal homepage](#) for more

Download details:

IP Address: 129.252.86.83

The article was downloaded on 29/05/2010 at 17:30

Please note that [terms and conditions apply](#).

# A new behaviour of ac losses in superconducting $\text{Bi}_2\text{Sr}_2\text{CaCu}_2\text{O}_8$ single crystals

S P Chockalingam<sup>1,4</sup>, S Sarangi<sup>1,5</sup>, S V Bhat<sup>1</sup>, K Oka<sup>2</sup>  
and Y Nishihara<sup>3</sup>

<sup>1</sup> Department of Physics, Indian Institute of Science, Bangalore 560012, India

<sup>2</sup> National Institute of Advanced Industrial Science and Technology, Tsukuba 3108152, Japan

<sup>3</sup> Faculty of Science, Ibaraki University, Mito 3108152, Japan

E-mail: [chocka@tifr.res.in](mailto:chocka@tifr.res.in)

Received 9 October 2008

Published 8 January 2009

Online at [stacks.iop.org/JPhysCM/21/045704](http://stacks.iop.org/JPhysCM/21/045704)

## Abstract

A new ac loss behaviour is observed in the superconducting state of  $\text{Bi}_2\text{Sr}_2\text{CaCu}_2\text{O}_8$  single crystals using a novel technique of measuring dissipation at radio frequencies. It is found that the ac loss in the superconducting state is larger than that in the normal state. This counter-intuitive result is explained in terms of the cumulative effect of repetitive decoupling of intrinsic Josephson junctions in the crystals and analysed in the framework of Ambegaokar–Baratoff theory. The ac losses are studied as a function of temperature, rf amplitude and magnetic field applied at different orientations. A peak in ac losses is observed in the superconducting state along the temperature scale. The amplitude of the peak decreases and shifts towards lower temperature with increasing field and also when the field orientation with respect to the  $c$  axis of the crystal changes from the perpendicular to parallel direction. The origin of the peak and its behaviour are discussed in the context of coupling energy of Josephson junctions present in the sample. In the presence of a magnetic field another peak in ac losses arises at temperatures close to  $T_c$ , which is associated with the Lorentz-force-driven motion of vortices.

(Some figures in this article are in colour only in the electronic version)

## 1. Introduction

Studies on ac losses in superconductors have been a subject of great interest for a long time not only as an important topic in fundamental science, but also as a basic requirement for the application of superconductors. A proper understanding of the mechanisms of ac losses and their quantitative knowledge is an essential requirement for any application. Such studies not only yield information on the material parameters crucial for applications but can also provide a test for any possible microscopic theory of superconductivity. As such there

has been a large number of reports on ac losses in the superconducting state [1–13]. By now it is established that ac losses in high  $T_c$  superconductors can arise from two sources: one is a Lorentz-force-independent mechanism such as weak link response [14], vortex–antivortex pair breaking [15], hysteresis [16], thermal effects [17], flux creep [18] and others [11]. The other one is Lorentz-force-driven motion of the vortices such as flux flow [19] and vortex motion [20]. Here we report a new behaviour in ac losses, which is different from the earlier studies. Generally in the superconducting state the dissipation is expected to be less when compared with that in the normal state. However, we observe that the ac losses in the superconducting state are larger than the normal state losses. Many reports are available on the ac losses at microwave frequencies [3–7] but studies at radio frequencies are considerably fewer [8, 9]. Many of these

<sup>4</sup> Author to whom any correspondence should be addressed. Present address: Department of Condensed Matter Physics, Tata Institute of Fundamental Research, Mumbai 400 005, India.

<sup>5</sup> Present address: Texas Center for Superconductivity, University of Houston, Houston, TX 77204, USA.

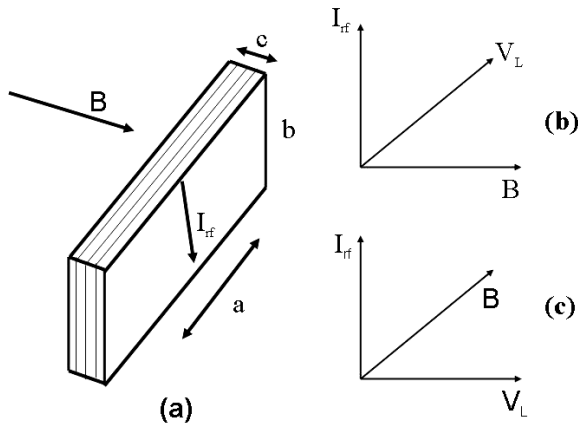


**Figure 1.** (a) Experimental configuration in which the external field is applied parallel to the  $c$  axis of the crystal ( $0^\circ$ ) perpendicular to which the superconducting layers are stacked in between the insulator layers. In this experimental arrangement the induced rf current flows along the  $a$ - $b$  plane. (b) Direction of the Lorentz force  $V_L$  when the field is parallel and (c) perpendicular to the  $c$  axis of the crystal.

studies have used the technique of non-resonant microwave and rf absorption. These techniques, though highly sensitive, give only the magnetic field derivative of the absorbed ac power.

In our studies we report the ac losses in superconducting  $\text{Bi}_2\text{Sr}_2\text{CaCu}_2\text{O}_8$  single crystals at radio frequencies determined from direct measurement of the absorbed power using an rf oscillator. The loss behaviour is strongly affected by the anisotropy of the sample, which is one of the distinctive properties of high  $T_c$  superconductors. The response of  $\text{Bi}_2\text{Sr}_2\text{CaCu}_2\text{O}_8$  single crystals is investigated as a function of temperature at different rf amplitudes and in the presence of a magnetic field applied at different angles with respect to the  $c$  axis of the crystal. The results are discussed in terms of a new model proposed by us [21], which explains ac losses as a consequence of the cumulative effect of energy spent in repetitive decoupling of the Josephson junctions in addition to Lorentz-force-driven motion of vortices.

## 2. Experimental details

The studies on ac losses described here have been made on air-annealed single crystals of  $\text{Bi}_2\text{Sr}_2\text{CaCu}_2\text{O}_8$ . The crystals were grown by the travelling zone flux method. The crystal which is used for the studies had a nominal  $T_c$  of  $\sim 85$  K with a narrow transition width ( $\Delta T \sim 1$  K) as determined by ac susceptibility measurements. The present studies of ac losses are carried out using an rf oscillator fabricated in our laboratory [22]. The oscillator consists of a self-resonant LC tank circuit driven by a NOT gate. The samples under investigation are placed in the core of an inductive coil forming the LC circuit whose resonant frequency is in the rf range. For the present work the frequency of the oscillator was kept around 8 MHz. The rf field in the coil induces an rf current in the sample, which changes according to the sample property. To maintain oscillations whenever there is a change in the rf current then the current drawn by the oscillator from the power supply also changes accordingly.

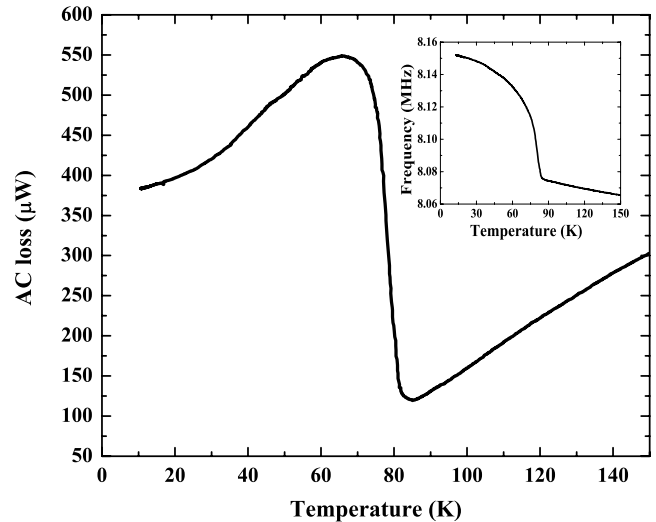


**Figure 2.** AC loss measured in  $\text{Bi}_2\text{Sr}_2\text{CaCu}_2\text{O}_8$  single crystal as a function of temperature in the absence of magnetic field with 5 V supply to the oscillator. The ac loss in the superconducting state is larger than that of normal state loss, and a peak-like behaviour is observed in ac loss in the superconducting state. The inset shows the change in the frequency of oscillations as a function of temperature. In the superconducting state the frequency of oscillations is more than that of the normal state.

The ac losses are calculated from the power absorbed by the sample in the presence of rf, which is determined from the measured change in total current supplied to the oscillator multiplied by the supply voltage. Typically we have used 5 V as the supply to the oscillator circuit. However, to investigate the ac loss behaviour at different rf amplitudes, studies are carried out with different supply voltages which in turn changes the amplitude of the rf field in the coil and hence the induced rf current [22].

A customized low temperature insert is used to integrate the experiment with a commercial cryostat and temperature controller along with a commercial electromagnet. The sample assembly can be rotated around the vertical axis to vary the angle  $\theta$  from  $90^\circ$  to  $0^\circ$  between the applied field and the  $c$  axis of the crystal. The sample is mounted inside the inductive coil with the  $c$  axis of the crystal perpendicular to the axis of the coil. In this experimental configuration the rf field induces rf current, as shown in figure 1(a). The magnetic-field-dependent measurements are carried out by applying the field at different orientations with respect to the  $c$  axis of the crystal. The orientation of the sample with respect to the coil axis and the induced current remains the same for different orientations of the sample assembly with respect to the applied field. But the direction of the Lorentz force that acts between the induced current and the external field varies according to the change in the orientation of the external field (figures 1(b) and (c)).

## 3. Results

The ac loss measured in the  $\text{Bi}_2\text{Sr}_2\text{CaCu}_2\text{O}_8$  single crystal as a function of temperature (150–10 K) in the absence of a magnetic field is shown in figure 2. In the normal state

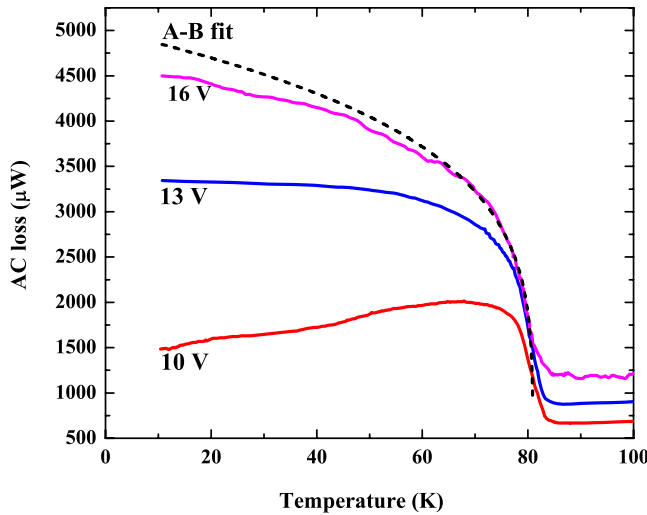


**Figure 3.** AC losses measured in  $\text{Bi}_2\text{Sr}_2\text{CaCu}_2\text{O}_8$  single crystal as a function of temperature in the absence of magnetic field with different rf currents obtained by varying the supply voltage to the circuit (10, 13 and 16 V) and loss calculated from the AB relation. Note the peak behaviour at 10 V and its absence at 13 and 16 V and the decreased deviation from the AB fit at 16 and 13 V.

the ac loss was found to decrease linearly with temperature. Quite unexpectedly, in the superconducting state the ac loss is observed to be more than that in the normal state. It is also found to increase with decreasing temperature, attain a peak and then decrease at further lower temperatures. The inset of figure 2 shows the corresponding change in the frequency of oscillations. In the normal state the frequency increases linearly with decreasing temperature and shows the transition into the superconducting state at 85 K through a sudden increase. Figure 3 shows the ac losses measured at different rf amplitudes obtained by varying the supply voltage. The losses are measured in the absence of magnetic field and with the supply voltages 10, 13 and 16 V. With increasing rf amplitude the ac loss increases. The loss at 10 V shows a peak-like behaviour similar to that obtained at 5 V as seen in figure 2. But at higher voltages, 13 and 16 V, the losses keep on increasing with decreasing temperature with the absence of any peak. When the temperature dependences of the ac losses are fitted to the Ambegaokar–Baratoff (AB) theory [23], the deviation of the observed ac losses from the fit is found to decrease with increasing rf amplitude and at 16 V the ac loss follows the AB behaviour quite well throughout the entire temperature range.

The ac losses as a function of temperature for different magnetic fields applied parallel to the  $c$  axis of the crystal is shown in figure 4(a). In the normal state, ac loss decreases with decreasing temperature without showing any field dependence. In the superconducting state two peaks, designated as A and B, are observed in the ac dissipation behaviour. The broad peak A arises at temperatures much below  $T_c$  and, on increasing the field, the amplitude of the peak decreases and the peak shifts towards lower temperature. The smaller hump-like peak B appears at higher temperature close to  $T_c$  and its amplitude increases with the magnetic field. The point P, as in figure 4(a), is considered as the minimum of two peaks and

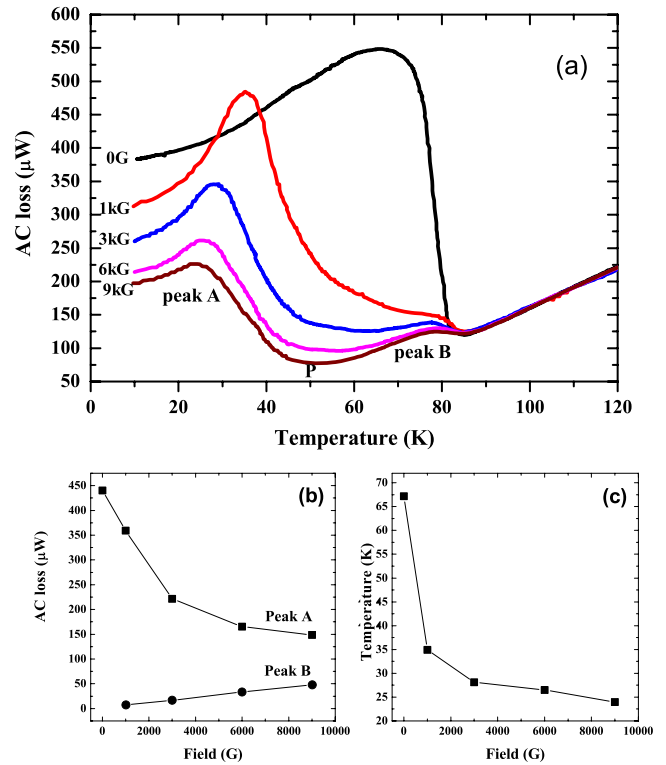


**Figure 4.** (a) AC losses measured in  $\text{Bi}_2\text{Sr}_2\text{CaCu}_2\text{O}_8$  single crystal as a function of temperature in the presence of different magnetic fields applied parallel to the  $c$  axis of the crystal. Two peaks, A and B, in ac losses are observed and the point P is taken to be the minimum of the two peaks from where the amplitude of the peaks is measured. (b) The changes in the amplitude of peaks A and B as a function of magnetic field. With increasing magnetic field the amplitude of peak A decreases. The amplitude of peak B increases linearly with increasing field. (c) Shift in the temperature at which the peak occurs for peak A as a function of the magnetic field. With increasing magnetic field the peak is shifted towards lower temperature.

the peak amplitudes are calculated with reference to this point. The amplitude of peak A is seen to decrease with increasing magnetic field whereas the amplitude of peak B increases linearly (figure 4(b)). The peak B appears at temperatures close to  $T_c$  and there is no significant shift in its position with changing field, whereas the position of peak A shifts towards lower temperatures with increasing field, as shown in figure 4(c).

In figure 5(a) the ac loss is shown as a function of temperature in the presence of a magnetic field of 6000 G applied at different angles  $\theta$  between the field and the  $c$  axis of the crystal at intervals of  $15^\circ$ . As the angle  $\theta$  changes from  $90^\circ$  to  $0^\circ$  the ac loss keeps on decreasing. At all orientations, the two peaks A and B in ac loss behaviour are observed except when the field is applied perpendicular to the  $c$  axis, where peak B disappears. The amplitude of peak A is maximum when the field is perpendicular to the  $c$  axis of the crystal and it drops sharply and decreases when the field orientation changes towards  $0^\circ$  (figure 5(b)). When the orientation changes from  $90^\circ$  to  $0^\circ$  peak A shifts towards lower temperature, as shown in figure 5(c), but the position of peak B remains unchanged with the change in orientation of the applied field. Figure 6

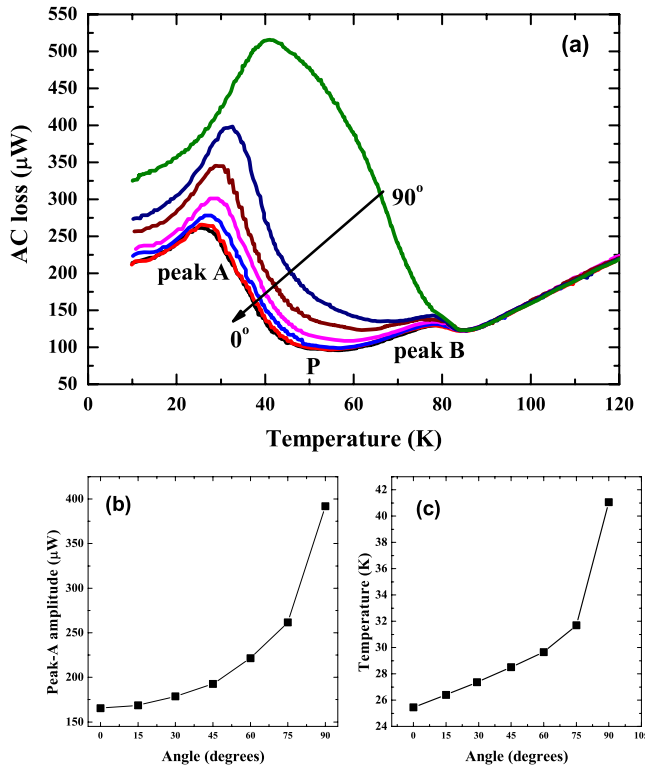


**Figure 5.** (a) Ac losses measured as a function of temperature in the presence of a magnetic field of 6000 G applied at different angles with respect to the  $c$  axis of the crystal. Note the decrease in the amplitude of peak A when the angle changes from  $90^\circ$  to  $0^\circ$  and its shift towards lower temperature and the increase in the amplitude of peak B. (b) Peak A amplitude as a function of the angle  $\theta$  between the field and the  $c$  axis. The amplitude decreases when  $\theta$  changes from  $90^\circ$  to  $0^\circ$  degrees and there is an abrupt drop in amplitude when the orientation changes from  $90^\circ$ . (c) Angular dependence of peak A position on the temperature scale. When  $\theta$  changes from  $0^\circ$  to  $90^\circ$  the peak is shifted towards high temperature and the shift is greater at  $90^\circ$  orientation.

shows the changes in the amplitude of peak B at different angles, which is decreasing when the orientation changes from  $0^\circ$  to  $90^\circ$  and vanishes at  $90^\circ$ . The results of rf loss studies on the  $\text{Bi}_2\text{Sr}_2\text{CaCu}_2\text{O}_8$  single crystal can be understood in terms of decoupling of Josephson junctions (JJ) in response to the induced rf current, applied field and temperature [21] and due to the losses arising out of Lorentz-force-driven vortex motion.

#### 4. Discussion

There are two types of Josephson junctions possible in the superconductors, as discussed below. In polycrystalline samples the micron size grains of relatively good stoichiometric crystalline material are separated by off-stoichiometric material (which may be weakly superconducting, non-superconducting but metallic, or even semiconducting or insulating). In this scenario, if the order parameter is sufficiently suppressed within the barrier, then the sample can be considered as an array of weak links which act as extrinsic Josephson junctions [9, 24, 25]. Also the extrinsic defects such as cracks, voids, segregated secondary phases and impurities lead to

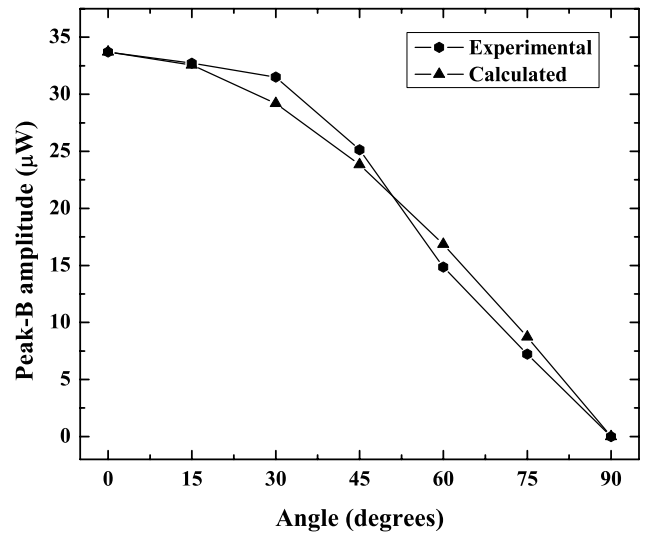


**Figure 6.** Peak B amplitude as a function of the angle  $\theta$  between the field and the  $c$  axis. The amplitude decreases when  $\theta$  changes from  $0^\circ$  to  $90^\circ$  degrees and the behaviour is fitted with the cosine of the orientation of the applied field with respect to the  $c$  axis.

the presence of Josephson junctions in the superconductors. In addition to this, one can also have Josephson junctions intrinsic to the crystal structure itself. This is because high- $T_c$  superconductors such as  $\text{Bi}_2\text{Sr}_2\text{CaCu}_2\text{O}_8$  have a layered crystal structure in which superconducting  $\text{CuO}_2$  planes are stacked alternately with non-superconducting or weakly superconducting interlayer. Because of this layered structure, the crystal structure itself acts as a continuous stack of Josephson junctions in which the bottom electrode of one junction acts as the top electrode for the next junction [26–29].

The Josephson junctions (whether intrinsic or extrinsic) have a characteristic coupling energy  $E_J$  given by  $E_J = \Phi_0 I_c / 2\pi$ , where  $\Phi_0$  is the flux quantum and  $I_c$  is the critical current of the junction, which is a measure of how strongly the phases of the two superconducting electrodes are coupled through the weak link [30–32]. When the sample is exposed to an rf field, an rf current is induced in it. For induced currents less than  $I_c$  the Josephson junction is in the steady state or zero voltage state, where the phase-locking between the superconducting layers is established. Then solutions of the form  $I = I_c \sin \varphi$  (Josephson first equation) determines the phase difference  $\varphi$  across the junction for a given applied current and there is no dissipation under this condition. If the induced rf current exceeds  $I_c$  for a given  $T$  and  $H$ , then the junction absorbs energy and gets decoupled [32] (phases get unlocked). The decoupled junction enters into the so-called running state or resistive state where dissipation occurs. In the resistive state the voltage  $V$  developed across the junction due to the time evolution of the phase difference in the junction is given by the Josephson second equation:

$$V = \frac{\Phi_0}{2\pi} \frac{d\varphi}{dt}. \quad (1)$$

The dynamic properties of the Josephson junction in the voltage or resistive state can be explained using the RCSJ



(resistively and capacitively shunted junction) model and tilted-washboard model [30–32]. In the RCSJ model the Josephson junction is modelled by an equivalent circuit consisting of a resistor  $R$  and a capacitor  $C$  in parallel with the Josephson junction. By summing all contributions to the current from all components, the total tunnelling current  $I_t$  flowing in the sample is given by

$$I_t = \frac{V}{R} + C \frac{dV}{dt} + I_c \sin \varphi. \quad (2)$$

The power dissipated by the junction in this resistive state is given by the product of the voltage  $V$  and the current  $I_t$  (equations (1) and (2)). The total power dissipated by the entire sample is given by the sum of the power dissipated by all the junctions in the resistive state ( $I_{rf} > I_c$ ). The dissipated power is emitted as high frequency radiation [27, 33].

The total energy dissipated by a Josephson junction is given by the sum of two terms: (1) the energy required to decouple the Josephson junction,  $E_J$ , and (2) the resistive state loss of the junction in the decoupled state. The point worth noting is that the JJ will absorb power and decouple only if  $I_{rf} > I_c$  at given  $T$  and  $H$ ; otherwise the JJ does not absorb any power and hence there will be no loss. With this model our results on  $\text{Bi}_2\text{Sr}_2\text{CaCu}_2\text{O}_8$  single crystals are satisfactorily explained as follows.

The highly anisotropic  $\text{Bi}_2\text{Sr}_2\text{CaCu}_2\text{O}_8$  single crystals, which contain superconducting  $\text{CuO}_2$  double layers forming superconducting electrodes of thickness  $3 \text{ \AA}$  and separated by insulating  $\text{Bi}_2\text{O}_3$  and  $\text{SrO}$  layers of thickness  $12 \text{ \AA}$ , could be considered as a stack of intrinsic Josephson junctions [26, 27]. In the presence of an rf field, when the sample attains the superconducting state, the Josephson junctions whose critical current is less than the induced current ( $I_c < I_{rf}$ ) gets decoupled and enter into the resistive state. Among the two contributions to the power loss in the single crystals as discussed above, the power loss due to the decoupling of JJ dominates over the contribution from the resistive state loss. In the resistive state the dissipated power is typically only of the order of a few picowatts as reported earlier [27, 33], which is much smaller than the observed dissipation. So the power dissipation observed here arises mainly due to the decoupling of JJ and the results are discussed on this basis.

In an ac cycle, the amplitude of the induced rf current in the sample changes continuously at a rate that depends on the frequency of oscillations. When the rf amplitude becomes more than the critical current of the Josephson junction, the junction absorbs energy and enters into the resistive state. Once the rf amplitude decreases below the critical current, the junction emits the same amount of energy in the form of heat and enters into the superconducting state. In one ac cycle the JJ is coupled and decoupled twice and this continuous decoupling and coupling leads to ac loss. The power absorbed or dissipated by the Josephson junctions present in the sample per second is given by the following expression [21]:

$$P = 2f \sum^N E_J \quad (3)$$

where  $f$  is the frequency of the rf current,  $N$  is the number of Josephson junctions in the sample with  $I_c < I_{rf}$  and  $E_J$

is the coupling energy of the JJ, which is expressed using the Ambegaokar–Baratoff theory [23] as

$$E_J(T, H) = \frac{\hbar}{2e} F(T) \left\langle I_0 \left| \frac{\sin(\pi \phi / \phi_0)}{(\pi / \phi_0)} \right| \right\rangle \quad (4)$$

where  $\phi$  is the flux produced by the magnetic field,  $\phi_0 = ch/2e$  is the flux quantum and  $F(T)$  is a factor dependent on temperature which is given by the AB theory as

$$F(T) = [\Delta(T)/\Delta(0)] \tanh[\Delta(T)/2K_B T] \quad (5)$$

where  $\Delta(T)$  is the temperature-dependent gap parameter and  $\Delta(0)$  is the gap at  $T = 0$ ;  $I_0$  is the maximum Josephson current given by

$$I_0 = \pi \Delta(0)/e R_n \quad (6)$$

where  $R_n$  is the normal state resistance of the junction;  $\phi = HA_J$  and  $A_J$  is the effective field penetration junction area orthogonal to  $H$ .

As seen from equation (3), the power absorbed at a given frequency depends both on the total number of junctions going into the resistive state and the strength of the individual junction. In our earlier studies [21, 22] we had observed that the loss in the superconducting state of ceramic YBCO increases with decreasing temperature. Even though the coupling energy of the intergranular extrinsic junctions of the ceramic sample was low, total power absorbed was large in the superconducting state, since the total number of such junctions was very large. In the present case, the coupling strength of each of these junctions is very high compared to that of the extrinsic junctions. Therefore a large power dissipation, more than that in the normal state, is observed. It should be noted that in a perfect crystal there should be no variation in the critical current between layers. However, in a real sample faults or defects in the crystal structure and variations in oxygen concentration from layer to layer can lead to variations in the critical current of Josephson junctions present in the sample [34]. Therefore the Josephson junctions have different coupling energies, thus leading to a distribution of the critical current  $I_c$  as discussed in the earlier reports [27, 35]. The number of JJ decoupled at different temperatures is different because the sample consists of a large number of JJ with a range of coupling strengths.

As shown in figure 2, when the sample enters into the superconducting state, the loss becomes more than the normal state loss due to the decoupling of Josephson junctions as discussed above. With the decreasing temperature the coupling energy of each JJ increases and more power is required for decoupling. Therefore the absorption of power also keeps on increasing with the decreasing temperature and reaches a maximum as seen in figure 2. Beyond this maximum, as the critical current of the Josephson junctions increases, the number of decoupling junctions decreases because the critical current becomes more than the induced current in the remaining junctions ( $I_c < I_{rf}$ ). The dissipation does not fall to zero beyond the maximum, which can be expected only in a perfect crystal where all the junctions would have the same coupling strength. Since the sample consists of Josephson junctions having different critical currents, the applied rf

field decouples weaker junctions having critical current less than the induced current and leads to dissipation. Therefore with decreasing temperature, as the strength of the junctions increases, the number of JJ with critical current less than the induced current ( $I_c < I_{rf}$ ) decreases. Therefore power absorption starts decreasing due to the decrease in the number of decoupled JJ. This leads to the observed peak-like behaviour in the ac losses as seen in figure 2. When the sample is in the normal state, the frequency of the oscillator increases linearly with decreasing temperature. The resistance of the coil  $L$  decreases with decreasing temperature, which reduces the damping factor of the oscillator and shifts the resonant frequency. At the transition temperature, the inductance in the oscillator decreases [4] due to the diamagnetic state of the sample and the frequency of the oscillator shows a transition as shown in the inset of figure 2. The increase in frequency leads to an increase in power dissipation as in equation (4), but this increase in dissipation is small and therefore cannot be responsible for the huge loss observed in the superconducting state.

The ac dissipation at different rf amplitudes is compared with Ambegaokar–Baratoff (AB) behaviour (figure 3), as discussed in the above model [21]. At lower rf amplitudes the observed ac losses deviate from the AB behaviour because the induced rf current is less and not able to decouple all the JJ, due to the increase in their coupling energy with decreasing temperature. With increasing voltages, the ac loss increases and this indicates that at higher rf currents a larger number of JJs are decoupled [35]. When the voltage is 10 V the ac loss behaviour has a peak similar to that of 5 V as in figure 2. But with increasing rf currents the behaviour changes. At higher voltages of 13 and 16 V there is no peak behaviour like at smaller rf amplitudes and for these voltages the behaviour also follows the AB fit. At higher rf currents the applied power is able to break stronger JJ with higher coupling energies, which were not decoupled earlier with smaller rf currents. When most of the JJ decouple there will not be any decrease in the ac loss at lower temperature. Therefore when the supply voltage is 16 V, the observed ac loss follows the AB fit with less deviation. Another possible reason for the absence of exact fitting with the AB function arises due to the presence of Josephson junctions with different coupling energies in the sample, which is different from the AB function that deals with single JJ as reported earlier [21].

The presence of a magnetic field weakens superconductivity and the strength of Josephson junctions. In the presence of a magnetic field, in addition to peak A, another peak (peak B) appears in ac loss behaviour (figure 4(a)). This is a consequence of the losses having two different origins: Josephson junction decoupling and Lorentz-force-driven motion of vortices. Peak A arises due to the power dissipated by JJ decoupling and it appears even in the absence of a magnetic field as discussed above. The coupling energy of JJ and hence the critical current  $I_c$  decreases with increasing magnetic field as given in equation (4). In the presence of the magnetic field, with the absorption of a lower amount of power, the junctions get decoupled and hence the ac loss decreases. With increasing magnetic field the amplitude

of peak A decreases and its position shifts towards lower temperature. The amplitude of peak A continuously decreases as shown in figure 4(b), which reflects the decrease in the coupling energy and hence the critical current  $I_c$  of JJ [27]. In this measurement the critical current dependence on magnetic field does not show a Fraunhofer pattern due to the presence of vortices and the distribution of JJ with different coupling energies. In the presence of magnetic field even at lower temperatures, a greater number of JJ have critical current less than the applied rf current ( $I_c < I_{rf}$ ) due to the decrease in the coupling strength of those junctions. Therefore peak A shifts towards lower temperature with increasing field as shown in figure 4(c).

The other peak (peak B) in ac losses appears just below  $T_c$  as shown in figure 4(a). In the absence of a magnetic field (figures 2 and 3) there is no peak-like behaviour arising close to  $T_c$ , which appears only in the presence of the magnetic field. The peak B arises in the presence of a magnetic field due to the Lorentz-force-driven vortex motion. Due to the external applied field  $B$  and induced rf current  $I_{rf}$  along the  $a$ – $b$  plane, a Lorentz force ( $I_{rf} \times B$ ) acts on the vortices which leads to vortex motion, which dissipates power. At temperatures close to  $T_c$  the vortices are not strongly pinned and they lead to dissipation due to the Lorentz-force-driven motion. With decreasing temperature, the pinning force of vortices becomes larger than the Lorentz force and the vortices get pinned. Therefore the dissipation due to their motion starts decreasing [36], and the peak-like behaviour appears just below  $T_c$ . Figure 4(c) shows the changes in the amplitude of peak B at different applied magnetic fields parallel to the  $c$  axis. With increasing field, the dissipation due to vortices increases because of the increase in the Lorentz force ( $I_{rf} \times B$ ). Therefore an increase in the amplitude of peak B with field is observed. Also, as discussed in earlier reports [37], the dissipation due to vortices increases linearly with the field (figure 4(c)).

The ac losses not only depend on the applied magnetic field but also on its orientation. The amplitude of peak A decreases and its position shifts towards lower temperatures when the angle between the applied field and the  $c$  axis of the sample changes from  $90^\circ$  to  $0^\circ$ , as shown in figure 5(a). This behaviour is explained as follows: the normal state resistance of the  $\text{Bi}_2\text{Sr}_2\text{CaCu}_2\text{O}_8$  single crystal is small in the  $a$ – $b$  plane and large along the  $c$  axis. According to the Ambegaokar–Baratoff relation the critical current density of a Josephson junction is inversely proportional to normal state resistance [23] so when the field is parallel to the  $c$  axis  $I_c$  is less and when the field is perpendicular to the  $c$  axis  $I_c$  is large and the power dissipation is more. In other words, as discussed earlier, the single crystals are made up of a stacking of strong and weak superconducting layers. When the field is applied perpendicular to the  $c$  axis the flux lines are injected parallel to the CuO layers and are strongly pinned in the weak superconducting layers. In this orientation the field penetrates the sample without weakening the superconducting property of the sample and thus the strength of the JJ coupling is not affected by the magnetic field. Thus the critical current density is maximum at this orientation and it decreases for other orientations as described in the literature [38–41]. The change

in the amplitude of peak A as a function of the orientation of the applied field is shown in figure 5(b). When the field is parallel to the  $c$  axis the flux pinning is least and the coupling energy of JJ is reduced by the applied field. Therefore the JJ needs less power to decouple and therefore the amplitude of peak A is low at this orientation. When the orientation of the field changes from  $90^\circ$  to  $0^\circ$ , the pinning in the weak superconducting layers decreases and so do the critical current [27] and the amplitude of peak A. But when the direction of the magnetic field is slightly away from the orientation perpendicular to the  $c$  axis, the critical current density and peak amplitude drastically decrease due to the existence of strong pinning centres parallel to the layers [39]. The shift in peak A position towards low temperature when the orientation of the field changes from  $90^\circ$  to  $0^\circ$  (figure 5(c)) indicates that the coupling energy of JJ and its critical current  $I_c$  decrease when the orientation changes from  $90^\circ$  to  $0^\circ$  and the shift is very large at  $90^\circ$  due to the strong pinning at this orientation. The intrinsic Josephson junction's critical current dependence on the magnetic field and its orientation was reported earlier by Kleiner and Muller [27] and the observed ac loss behaviour matches their results.

In high  $T_c$  layered superconductors, particularly in highly anisotropic materials like  $\text{Bi}_2\text{Sr}_2\text{CaCu}_2\text{O}_8$ , the superconductivity is treated as 2D rather than 3D. In this material the magnetic field penetrates as pancake vortices when the field is parallel to the  $c$  axis and as Josephson vortices when perpendicular. In other orientations the pancake vortices are connected through Josephson strings. In our studies we observe the maximum amplitude of peak B, when the field is parallel to the  $c$  axis, and that the peak nearly vanishes at perpendicular orientation. As shown in figures 1(b) and (c), the rf current flows in the  $a$ - $b$  plane of the crystal and the Lorentz force acts on the vortices in the presence of a magnetic field. When the field is applied parallel to the  $c$  axis, the applied field penetrates as pancake vortices and the Lorentz force acts in the  $a$ - $b$  plane along the  $a$  axis. Therefore the vortices move in the  $a$ - $b$  plane in the direction of the Lorentz force (figure 1(b)) which leads to dissipation. In the perpendicular orientation the field penetrates along the  $a$ - $b$  plane as Josephson vortices and the Lorentz force acts along the  $c$  axis as seen in figure 1(c). However, the movement of the vortices in this orientation is not favourable due to the strong pinning of vortices in between the superconducting planes and the dissipation is less [18]. When the applied field changes from parallel orientation ( $90^\circ$ - $0^\circ$ ), the vortices get pinned and the dissipation decreases following the cosine of the field orientation. The good fit of the data with calculated values, as seen in figure 6, confirms that the peak arises due to vortex motion. There is no significant shift in the position of peak B at different amplitudes of the magnetic field and its orientation as shown in figures 4(a) and 5(a). This shows that, at the relatively low magnetic fields as used in our studies, the vortices get depinned only at high temperatures.

In conclusion, we have observed apparently unusual larger than normal state ac losses in superconducting single crystals of  $\text{Bi}_2\text{Sr}_2\text{CaCu}_2\text{O}_8$  and have investigated the loss behaviour at different rf amplitudes and magnetic fields applied at different orientations. We observed two peaks A and B in power dissipation as a function of temperature. The studies on ac

losses as a function of magnetic field applied at different orientations reveals that peaks arise due to JJ decoupling and the vortex motion. With increasing magnetic field the peak A amplitude decreases and when the orientation changes from  $0^\circ$  to  $90^\circ$  the amplitude increases. This is explained in terms of critical current density corresponding to the coupling energy ( $E_J$ ) of the JJ. The peak B amplitude increases with field and decreases when the angle changes from  $0^\circ$  to  $90^\circ$  and vanishes at  $90^\circ$  and is explained in terms of the Lorentz-force-driven motion of vortices.

## Acknowledgments

We thank Ms Madhavi Chand for help in the preparation of this paper. This work is supported by the Department of Science and Technology and University Grants Commission, Government of India.

## References

- [1] Carr W J 1983 *AC Loss and Macroscopic Theory of Superconductivity* (New York: Gordon and Breach)
- [2] Amemiya N, Jiang Z, Iijima Y, Kakimoto K and Saitoh T 2004 *Supercond. Sci. Technol.* **17** 983
- [3] Bhat S V 1996 *Studies of High Temperature Superconductors* vol 18, ed A V Narlikar (New York: Nova Science) p 241
- [4] Bhat S V, Ganguly P, Ramakrishnan T V and Rao C N R 1987 *J. Phys. C: Solid State Phys.* **20** L559
- [5] Rastogi A, Sudershan Y S, Bhat S V, Grover A K, Yamaguchi Y, Oka K and Nishihara Y 1996 *Phys. Rev. B* **53** 9366
- [6] Rao C N R, Vijayaraghavan R, Ganapathi L and Bhat S V 1989 *J. Solid State Chem.* **79** 177
- [7] Purnell A J, Cohen L F, Zhai H Y, Christen H M, Paranthaman M P, Lownders D H, Hao L and Gallop J C 2004 *Supercond. Sci. Technol.* **17** 681
- [8] Wang Z, Leigh J S Jr, Wickiund S and Stein A 1998 *Supercond. Sci. Technol.* **1** 24
- [9] Sudershan Y S, Rastogi A, Bhat S V, Grover A K, Yamaguchi Y, Oka K and Nishihara Y 1998 *Physica C* **297** 253
- [10] Bonin B and Safa H 1991 *Supercond. Sci. Technol.* **4** 257
- [11] Kadowaki K, Songaliu Y and Kitazawa K 1994 *Supercond. Sci. Technol.* **7** 519
- [12] Nguyen P P, Oates D E, Dresselhaus G, Dresselhaus M S and Anderson A C 1995 *Phys. Rev. B* **51** 6686
- [13] Luo H, Wu X F, Lee C M, Yang Y, Leng X, Liu Y, Qiu L, Luo H M, Wang Z H and Ding S Y 2002 *Supercond. Sci. Technol.* **15** 370
- [14] Patanjali P V and Seshu Bai V 1998 *Physica C* **301** 192
- [15] Ando Y, Motohira N, Kitazawa K, Takeya J-I and Akita S 1991 *Phys. Rev. Lett.* **67** 2737
- [16] Zannella S, Jansak L, Majoros M, Selvamanickam V and Salama K 1993 *Physica C* **205** 14
- [17] Palstra T T M, Batlogg B, Schneemeyer L F and Waszczak J V 1988 *Phys. Rev. Lett.* **61** 1662
- [18] Kim J-J, Lee Ho-K, Chung J, Shin H J, Lee H J and Ku J K 1991 *Phys. Rev. B* **43** 2962
- [19] Kwok W K, Welp U, Crabtree G W, Vandervoort K G, Hulscher R and Liu J Z 1990 *Phys. Rev. Lett.* **64** 966
- [20] Sabharwal S C, Gupta S K, Gupta M K and Pinto R 1995 *Physica C* **245** 386
- [21] Sarangi S, Chockalingam S P and Bhat S V 2005 *J. Appl. Phys.* **98** 073906
- [22] Sarangi S and Bhat S V 2005 *Rev. Sci. Instrum.* **76** 023905
- [23] Ambegaokar V and Baratoff A 1963 *Phys. Rev. Lett.* **10** 486



- Ambegaokar V and Baratoff A 1963 *Phys. Rev. Lett.* **11** 104
- [24] Prester M 1998 *Supercond. Sci. Technol.* **11** 333
- [25] Marcon R, Fastampa R, Giura M and Maticotta C 1989 *Phys. Rev. B* **39** 2796
- [26] Kleiner R, Steinmeyer F, Kunkel G and Muller P 1992 *Phys. Rev. Lett.* **68** 2394
- [27] Kleiner R and Muller P 1994 *Phys. Rev. B* **49** 1327
- [28] Rapp M, Murk A, Semerad R and Prusseit W 1996 *Phys. Rev. Lett.* **77** 928
- [29] Uematsu Y, Mizugaki Y, Nakajima K, Yamashita T, Watauchi S and Tanaka I 2002 *Physica C* **367** 382
- [30] Bok J (ed) 1998 *The Gap Symmetry and Fluctuations in High Temperature Superconductors* (New York: Plenum)
- [31] Tinkham M 1996 *Introduction to Superconductivity* (New York: McGraw-Hill)
- [32] Poole C, Farach H A and Creswick R J 1995 *Superconductivity* (New York: Academic)
- [33] Batov E, Jin X Y, Shitov S V, Koval Y, Muller P and Ustinov A V 2006 *Appl. Phys. Lett.* **88** 262504
- [34] Yurgens A, Winkler D, Claeson T, Yang G, Parker I F G and Gough C E 1999 *Phys. Rev. B* **59** 7196
- [35] Suzuki M, Watanabe T and Matsuda A 1998 *Phys. Rev. Lett.* **81** 4248
- [36] Blatter G, Geshkenbein V B, Larkin A I and Vinokur V M 1994 *Rev. Mod. Phys.* **66** 1125
- [37] Matsuda Y, Shibata A, Izawa K, Ikuta H, Hasegawa M and Kato Y 2002 *Phys. Rev. B* **66** 014527
- [38] Roas B, Schultz L and Saemann Ischenko G 1990 *Phys. Rev. Lett.* **64** 479
- [39] Tachiki M and Takahashi S 1989 *Solid State Commun.* **72** 1083
- [40] Kes P H, Aarts J, Vinokur V M and VanderBeek C J 1990 *Phys. Rev. Lett.* **64** 1063
- [41] Schmitt P, Kummeth P, Schultz L and Saemann-Ischenko G 1991 *Phys. Rev. Lett.* **67** 267